

TRANSIENT SIMULATION CALCULATION FOR ELECTRIC THERMAL ANTI-ICING PERFORMANCE OF COMPOSITE WING IN ICING ENVIRONMENT

Zheyuan Dong¹, Xiaofeng Guo¹, Wei Dong¹ & Pingyang Wang¹

¹ School of Mechanical Engineering, Shanghai Jiao Tong University, China

Abstract

One-dimensional transient simulation on the electric anti-icing of composite material wings is conducted where the heat transfer of surface freezing and evaporating phase is considered. By numerically calculating the thickness of the external ice layer and water layer during the electric heating process under icing conditions, we can observe the real-time effect of electric anti-icing, and the effect of electric anti-icing under different heating conditions is obtained. From this, the most suitable heating and anti-icing scheme can be determined based on different external flow conditions and wing icing conditions.

Keywords: electrothermal anti-icing system, composite material, phase change heat transfer, transient simulation

1. Introduction

Icing can significantly affect the aerodynamic performance of an aircraft, it affects the stability of the aircraft and form a safety hazard. Therefore, it is necessary to take effective anti-icing measures or install corresponding anti-icing systems in frozen region. In order to reduce the weight of the aircraft, the fuselage and wings are widely made of carbon fiber reinforced resin matrix composites. For the electric heating device, the anti-icing system uses an ultra-thin flexible heating film embedded in a carbon fiber reinforced resin matrix composite laminate [1]. The use of electric heating anti-icing system has a high reliability and installation flexibility, which can effectively prevent icing, and can significantly improve flight safety when flying under icing conditions [2]. Therefore, it has a broad application prospect in the anti-icing system of carbon fiber composite wings.

Since this physical process includes a series of thermal conductivity, phase transformation, flow and other problems, it is difficult to predict the heating process and evaluate the anti-icing effect. In the flight process, it is necessary to select a reasonable heating method according to the current situation to keep the ice thickness less than a certain thickness in a certain period of time, when the impact on the flight is acceptable.

The research finished by Xiaofeng Guo and Qian Yang focuses on optimizing the power distribution for electrothermal anti-icing systems. The study uses differential evolution algorithm to minimize power consumption while ensuring effective anti-icing. The algorithm optimizes the heating element layout to prevent runback water to enhance the system's efficiency [3]. The results demonstrate significant improvements in power efficiency and anti-icing performance.

The numerical research on electric deicing is mainly divided into several main parts. The first part focuses on a series of processes related to impact, overflow, freezing, melting, and evaporation caused by external environmental effects on the wing surface. Silva et al. obtained empirical formulas related to convective heat transfer in laminar and turbulent flow by coupled calculating the external air flow and water film flow [4][5]. Bu et al. obtained the steady-state anti-icing process of the electric heating anti-icing system based on the known electric heating power, which is consistent with the experiment [6]. Shen calculated the transient anti-icing process, ignoring the influence of the ice layer on the flow field. He introduced a freezing fraction based on the anti-icing temperature to calculate

TRANSIENT SIMULATION CALCULATION FOR ELECTRIC THERMAL ANTI-ICING PERFORMANCE OF COMPOSITE WING

the coupling between the flow field and solid thermal conductivity in a single time step [7]. Mu et al. developed a transient coupled numerical heat transfer model for an electric anti-icing system, which includes water film flow [8]. The phase transition process is iteratively solved after appropriate thermal boundary conditions are met to determine the heat distribution and ice shape, applying the convective heat transfer coefficient and water collection coefficient from steady-state results.

In addition to continuous heating, there are also periodic heating methods for electric anti-icing. Ding conducted numerical calculations on the periodic electric heating anti-icing system of the hood and calculated the minimum energy consumption to maintain an ice free state, demonstrating that periodic heating can avoid overheating and improve energy efficiency under the same average power [9]. Chang uses different heat distribution methods to search for the flow state and temperature limits of the incoming flow under the condition of no ice formation on the surface, in order to demonstrate that different heat time and spatial distributions under the same average heat flux density are crucial for maintaining the maximum incoming flow conditions without ice formation [10]. In the anti-icing state, Pourbagian optimized the heating process through a reduced order model that includes time, using spatial and temporal distribution as control conditions [11].

2. Heat transfer models and numerical method of electrothermal anti-icing

2.1 The structure of electrical heating system

The structure of electrical heating system is shown in Figure 1.

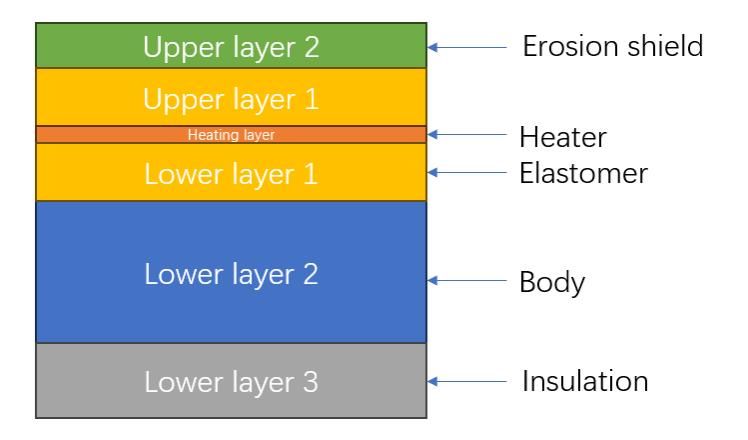


Figure 1 – Structure of electrical heating system

The physical properties of each layer are:

```
Erosion shield L=0.20mm, \lambda=16.3 \text{W/m} \cdot \text{K}, \rho=8025.25 kg/m^3, c=502.416 J/kg \cdot K

Heater L=0.013mm, \rho=8906.2 kg/m^3, c=385.186 J/kg \cdot K

Elastomer L=0.28mm, \lambda=0.256 \text{W/m} \cdot \text{K}, \rho=1348 kg/m^3, c=1256 J/kg \cdot K

Body L=0.89mm, \lambda=0.294 \text{W/m} \cdot \text{K}, \rho=1794 kg/m^3, c=1570.05 J/kg \cdot K

Insulation L=3.43mm, \lambda=0.121 \text{W/m} \cdot \text{K} \cdot s, \rho=648.75 kg/m^3, c=1130.44 J/kg \cdot K
```

On the surface of the wing, the supercooled water droplets impact the surface of the wing, and the supercooled water droplets freeze and release phase transition heat. If the impact of the supercooled liquid water content (LWC) is relatively large, the supercooled water droplets cannot freeze completely, but some freeze and some form overflow water. When the anti-icing heat is transferred to the surface, the ice accumulation on the surface will melt. The water droplet impact and flow heat transfer on the wing surface are shown in Figure 2.

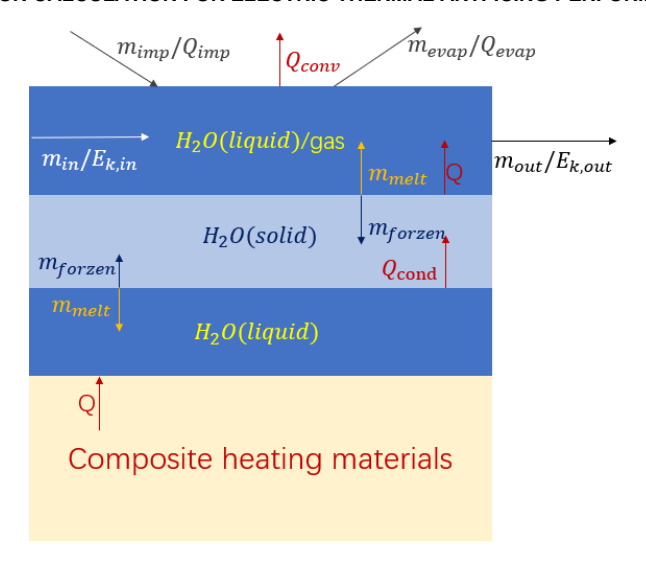


Figure 2 – Heat and mass exchange between layers

2.2 Physical model for numerical simulation

As the supercooled water \dot{m}_{imp} is added to the computational element through CFD calculation of incoming air, and obtains the thermal convection heat transfer coefficient h_c through incoming air velocity and LWC. The wing can be divided into several parts to calculate the fluid velocity in the computational element and the convective heat transfer coefficient at the local location.

Assuming that the evaporation area on the control calculation element is the same as the area where water droplets impact into the unit element, the mass of liquid water evaporation per unit area is:

$$\dot{m}_{evap} = h_m[\rho_{v,w}(T_w) - \rho_{v,e}]$$

where h_c is the convective heat transfer coefficient on the surface.

The mass transfer coefficient between the airflow and the water film is:

$$h_m = \frac{h_c}{\rho_a c_{n,a}} \left(\frac{Pr}{Sc}\right)^{\frac{2}{3}}$$

where h_m is the surface mass transfer coefficient when liquid water exists on the surface (the thickness of the surface water layer is not 0).

The density of water vapor in the incoming air and the density of surface vapor are determined by the gas state equation,

$$\rho_{v,w}(T_w) = \frac{p_{v,w}(T_w)}{R_v T_w} \quad \text{and} \quad \rho_{v,e} = \frac{p_{v,e}}{R_v T_e}$$

where the vapor pressure at a specific temperature $P_{v,w}$ and $P_{v,e}$ can be calculated from the Magnus formula:

$$p_v = p_0 \exp\left[\frac{18.75(T - 273.15)}{T - 38.25}\right]$$

By combining the above formula, it can be obtained that the evaporation mass per unit area on the surface of the water model is[12]:

$$\dot{m}_{evap} = \frac{h_c}{\rho_a c_{v,a}} (\frac{Pr}{Sc})^{\frac{2}{3}} [\frac{p_{v,w}(T_w)}{R_v T_w} - \frac{p_{v,e}}{R_v T_e}]$$

We focus on the formation of an outer ice surface and the conservation of mass and energy in solid-liquid-gas states.

Considering the water and ice layer as a whole, the energy conservation on the outer surface is given by.

$$\dot{H}_{imp} + \dot{H}_{ice} + \dot{H}_{in} + \dot{Q}_{cond} = \dot{H}_{evap} + \dot{Q}_{conv} + \dot{H}_{out}$$

where $[H_{\text{imp}} = m_{\text{imp}} \left(c_{p,w} T_o + \frac{u_{a,o}^2}{2} \right)]$ with velocity and temperature as inflow conditions.

Simplifying in one dimension, we can assume:

$$[H_{\text{out}}^{\cdot} = H_{\text{in}}]$$

The latent heat and enthalpy released by the freezing structure within the unit area are:

$$\dot{H}_{ice} = \dot{m}_{ice}(L_f - c_{p,w}T_f)$$

The conductive heat from the unit area on the wing surface is:

$$\dot{Q}_{cond} = \lambda_1 \frac{\partial T_1}{\partial x} |_{x=L1}$$

The enthalpy of unfrozen water leaving the control body per unit area is:

$$\dot{H}_{evap} = \dot{m}_{evap} (L_e - c_{p,w} T_w)$$

The convective heat flow per unit area caused by convection is:

$$\dot{Q}_{conv} = h_c (T_w - T_f)$$

The mass conservation of the control body is:

Similarly, we can assume:

$$[m_{\mathsf{in}} = m_{\mathsf{out}}]$$

Therefore, the increased mass is:

$$[\dot{m_{
m imp}} - \dot{m_{
m evap}} = \dot{m_{
m water}} + \dot{m_{
m ice}}]$$

The numerical solution for the heat conduction process is:

1) For the heating process of the heater, energy conservation equation,

$$\rho l \cdot c_p \frac{\partial T}{\partial t} - \lambda_1 \frac{\partial T_1}{\partial x} - \lambda_2 \frac{\partial T_2}{\partial y} = q$$

where (T) is the heater temperature, and (T_1) and (T_2) are the temperatures of the regions above and below the heater. This shows the heater temperature distribution.

- 2) The transient process is selected using the finite difference scheme of the general heat conduction equation.
- 3) The mass of the melting and evaporation process of the ice structure is solved by the combined mass and energy conservation:

$$\dot{m}_{imp}\left(c_{p,w}T_{\infty} + \frac{u_{d,\infty}^{2}}{2}\right) + \dot{m}_{ice}\left(L_{f} - c_{p,w}T_{f}\right) + \lambda_{1}\frac{\partial T_{1}}{\partial x}|_{x=L1} = \dot{m}_{evap}\left(L_{e} - c_{p,w}T_{w}\right) + h_{c}\left(T_{w} - T_{f}\right)$$

This is the result obtained when the solid and liquid are mixed, if there is only ice and no melting, all the enthalpy is converted to the ice and change the temperature of ice layer.

The above part is mainly a result of the overall conservation of energy and mass, and the fact that at any one time, the heat exchange between the ice sheet, the upper layer of water (which exists under special circumstances), the ice sheet, and the bottom layer of melting liquid water is satisfied:

$$\Delta h_c = Q_{in} - Q_{out}$$

If there exists upper water layer, then enthalpy change per unit area satisfies:

$$\Delta h_{c.water} = \rho l \cdot C p_{water} \cdot T_{water}$$

and mass change per unit area satisfies:

$$\rho \Delta l = m_{\rm imp} + m_{\rm melt} - m_{\rm evap}$$

The energy/enthalpy get in is:

$$Q_{in} = Q_{cond} + Q_{imn}$$

The energy/enthalpy get out is:

$$Q_{out} = Q_{conv} + Q_{evan}$$

For the ice layer, enthalpy change per unit area satisfies:

$$\Delta h_{c,ice} = -\gamma \cdot \rho \Delta l - \rho \Delta l \cdot C p_{ice} \cdot \overline{T_{ice}}$$

We assume the average ice temperature is the average of both side $\,$ (environment temperature and 273.15K) $\,$.

The mass change per unit area satisfies:

$$\rho \Delta l = -m_{\text{melt}} + m_{\text{frozen}}$$

The energy/enthalpy get in is:

$$Q_{in} = Q_{cond_ice} + H_{melt}$$

where H_{melt} consider the enthalpy of melting water below (or both sides).

The energy/enthalpy get out is:

$$Q_{out} = Q_{conv} + H_{frozen}$$

For the bottom water layer, enthalpy change per unit area satisfies:

$$\Delta h_{c,water} = \rho \Delta l \cdot C p_{water} \cdot \overline{T_{water}}$$

We assume the average water temperature is the average of both side (273.15K and wall temperature).

The mass change per unit area satisfies:

$$\rho \Delta l = m_{\text{melt}} - m_{\text{frozen}};$$

The energy/enthalpy get in is:

$$Q_{in} = Q_{cond} + H_{melt};$$

where H_{melt} consider the enthalpy of melting water below (or both sides).

The energy/enthalpy get out is:

$$Q_{in} = H_{melt} + Q_{cond_ice}.$$

The Q_{cond_ice} above is assumed through the convective thermal resistance of air (or water) and the thermal resistance of ice (using the temperature of environment).

2.3 Numerical method for transient simulation of anti-icing process

The flow chart for simulation is shown in figure 3.

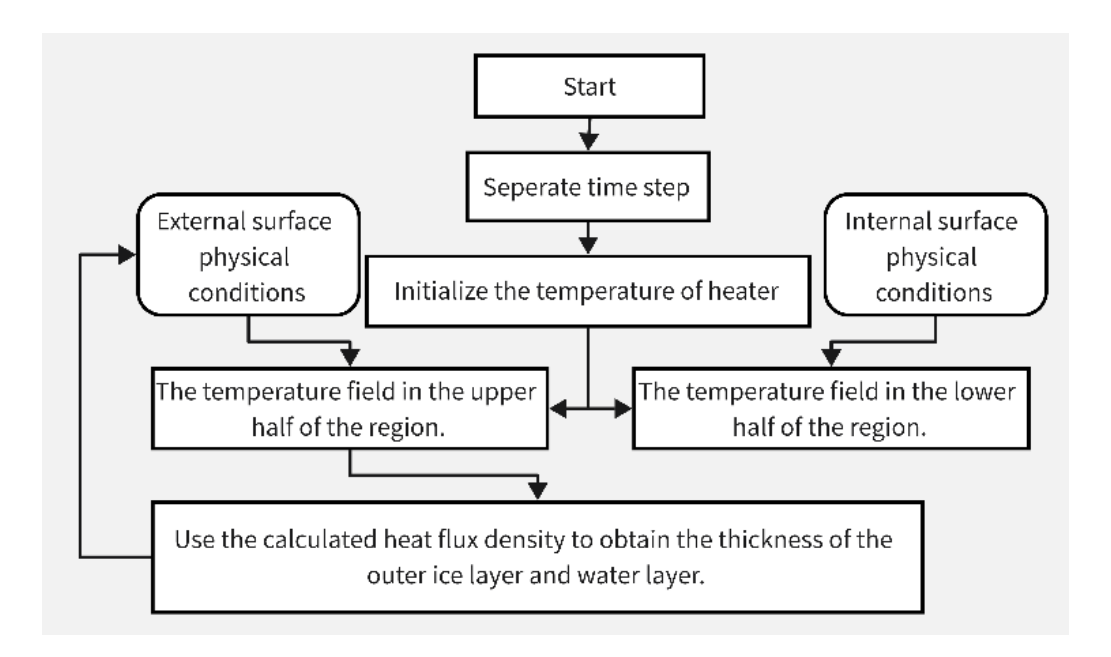


Figure 3 – Flow chart for simulation

For the convenience of ignoring the thermal conductivity process of the ice layer when the ice layer thickness is relatively thin, there is no need to perform differential analysis on the ice layer. If the ice layer is thick, the thermal conductivity process of the ice layer needs to be considered.

Due to the fact that the thickness will be 0 during the generation and melting evaporation processes of ice and water layers, the spatial difference step size for ice and water layers is very small, so an implicit format is recommended to be chosen. Fix the number of steps, which can be iterated over time to obtain a step size that varies over time.

At each time step, we update the heat transfer conditions on the upper surface of the wing based on the thickness of the ice and water layers from the previous moment, to reflect the impact of icing and melting on the heating environment of the wing itself.

For composite materials, as the thickness of layer is thin and the spatial difference is small, the time step the explicit format will be very small, which increases the computational cost. Therefore, implicit format should be chosen.

3. Simulation results and analysis

3.1 Numerical simulation of ant-icing under different heat flux

The simulation of anti-icing by electric heating is carried out at heat flux of 20kW, 30kW and 40kW for the inflow of -20° C and LWC of $1g/m^3$ and air velocity 50m/s. In the numerical calculation, the initial thickness of ice layer is 1mm.

The anti-icing performance and the transient change of the thickness of each layer over time are shown in the figure 4~6.

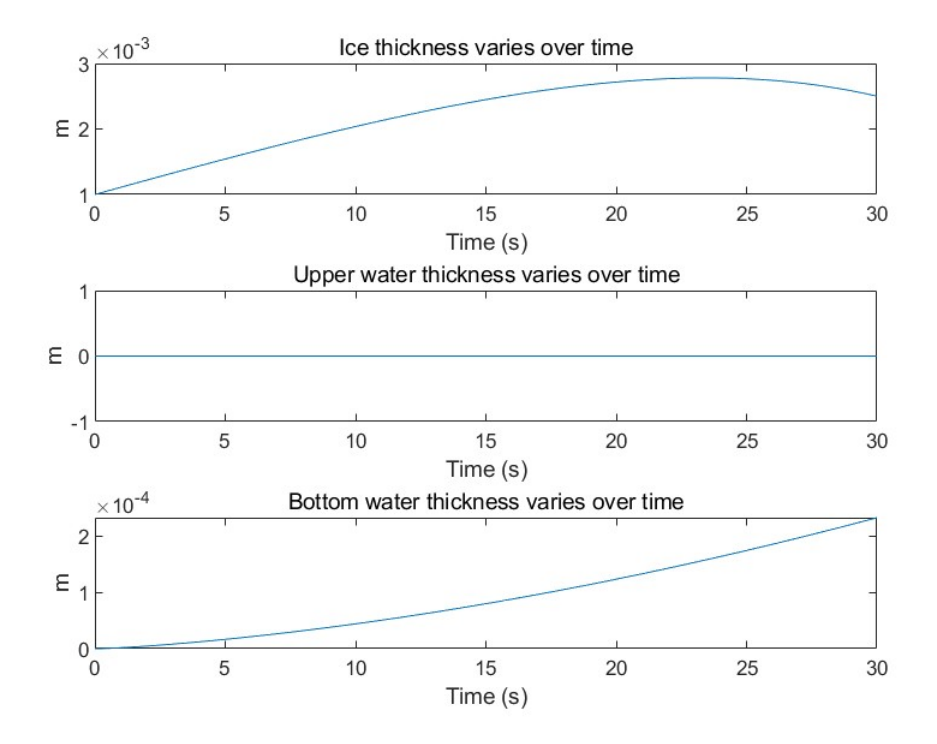


Figure 4 – 20kW heating condition

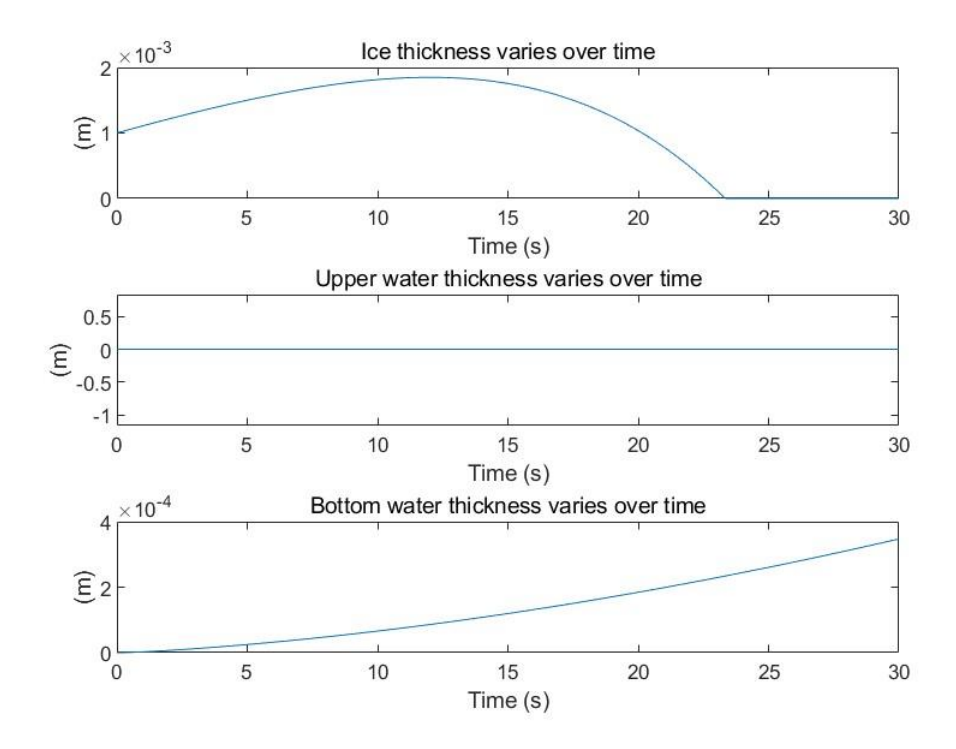


Figure 5 – 30kW heating condition

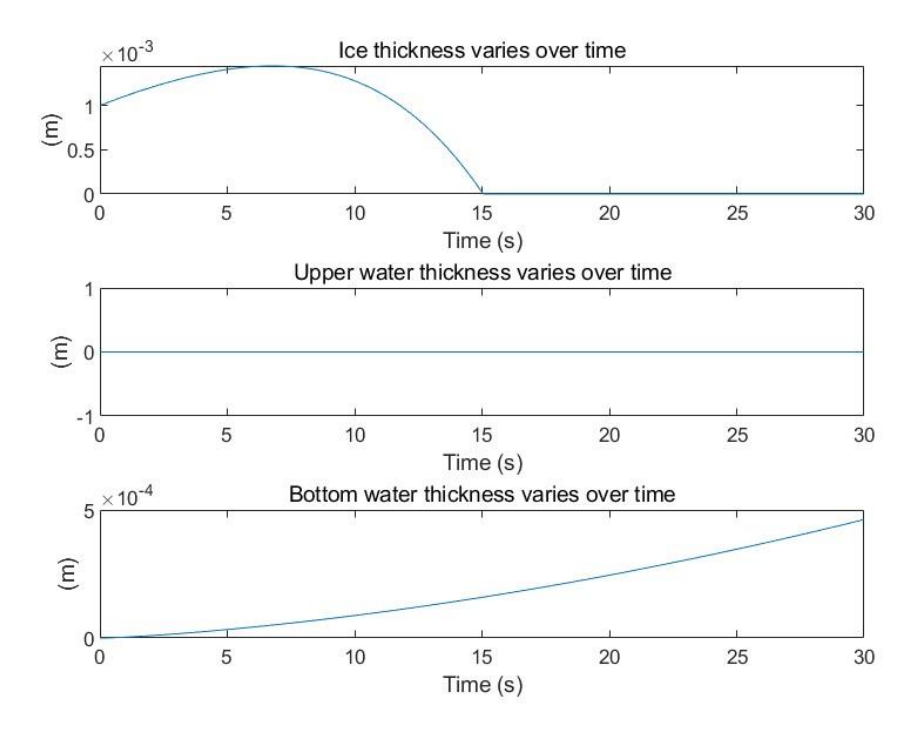


Figure 6 – 40kW heating condition

According to the results, under the continuous 20kW heat source, the ice layer has a melting trend, and with the increase of heat flux, the ice layer can be completely melted within 20 seconds at heat flux of 40kW,. And when the environment is -20° C, there is no upper water layer before the ice is completely melted.

If we denote the time between the change in the heating state and the time when the ice starts to reduce (lower than the initial condition) and the total decrease 'response time'. Then we can find that the response time is reduced as more heat flux is given. (20kW: >>30s; 30kW: 20.0s; 40kW: 11.5s)

3.2 Influence of environmental factors on anti-icing performance

3.2.1 The LWC (Liquid water content)

Under the same icing condition in 3.1 (velocity & environment temperature), fix the heat flux 20kW and vary the LWC from 0.25, 0.5, $1.0g/m^3$. The anti-icing results are shown in the figure 7~8, the condition $1.0g/m^3$ is shown in figure 4.

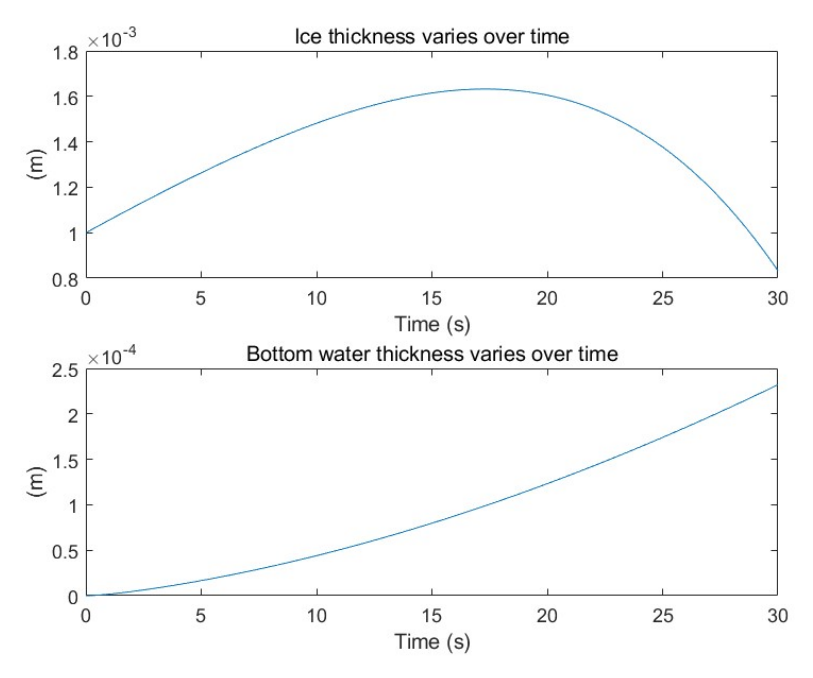


Figure 7 – 20kW LWC= $0.5g/m^3$

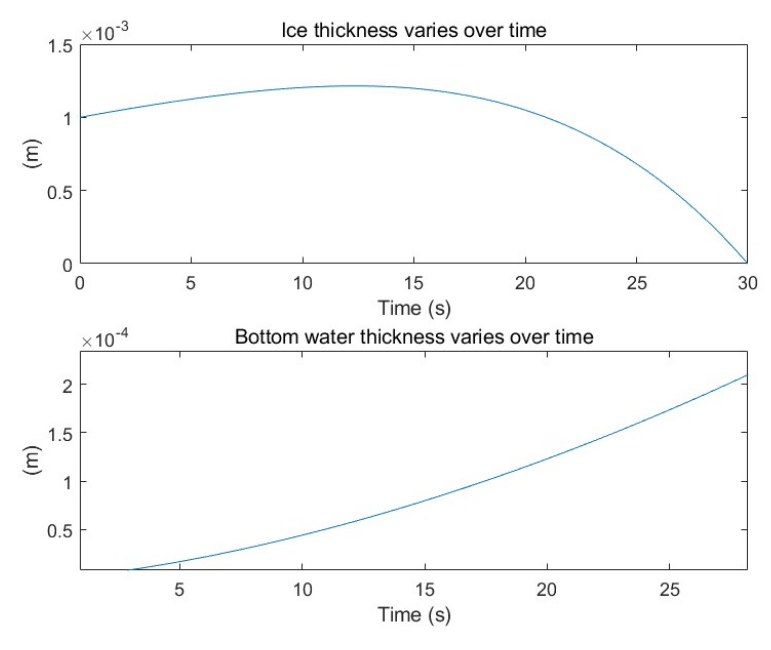


Figure 8 – 20kW LWC= $0.25g/m^{3}$

From the calculation, we can see that the liquid water content mainly affects the thickness of the ice sheet, and the influence on the thickness of the underlying water is not very big, only a little less than 10%. And the response time also decreases as the water content decreases. ($0.5g/m^3$:28.4s; $0.25g/m^3$:20.5s). Because the ice is thinner and melts faster at bottom water layer, the required thickness of the underlying water film is smaller and it takes less time to break off.

3.2.2 The environment temperature

Under the same condition in 3.1 (velocity & LWC), fix the heat flux 20kW and vary the environment temperature.

The anti-icing results are shown in the figure $9\sim11$, the condition -20° C is shown in figure 4

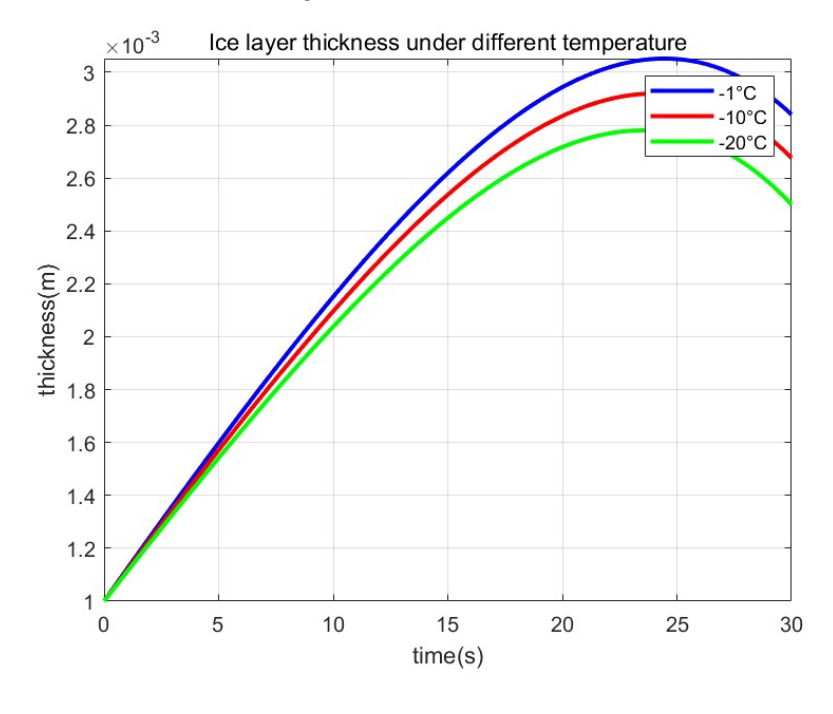


Figure 9 –The thickness of ice layer under different environment temperature

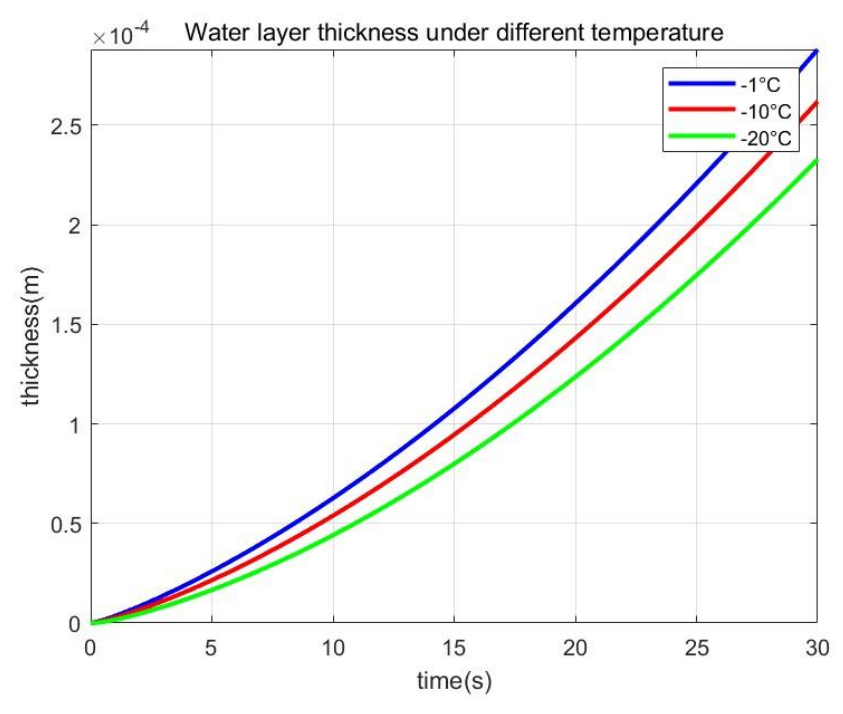


Figure 10 –The thickness of bottom water layer under different environment temperature

Under temperature -1° C, -20° C, there is no upper water layer, the surface supercooled water will freeze completely while hitting the ice surface. Under the fixed velocity, the temperature of the supercooled water after collision will not exceed the freezing point.

In these cases, the enthalpy of supercooled water does not have a significant amount of ice, as the majority of the enthalpy in supercooled water is converted to the temperature of the ice layer.

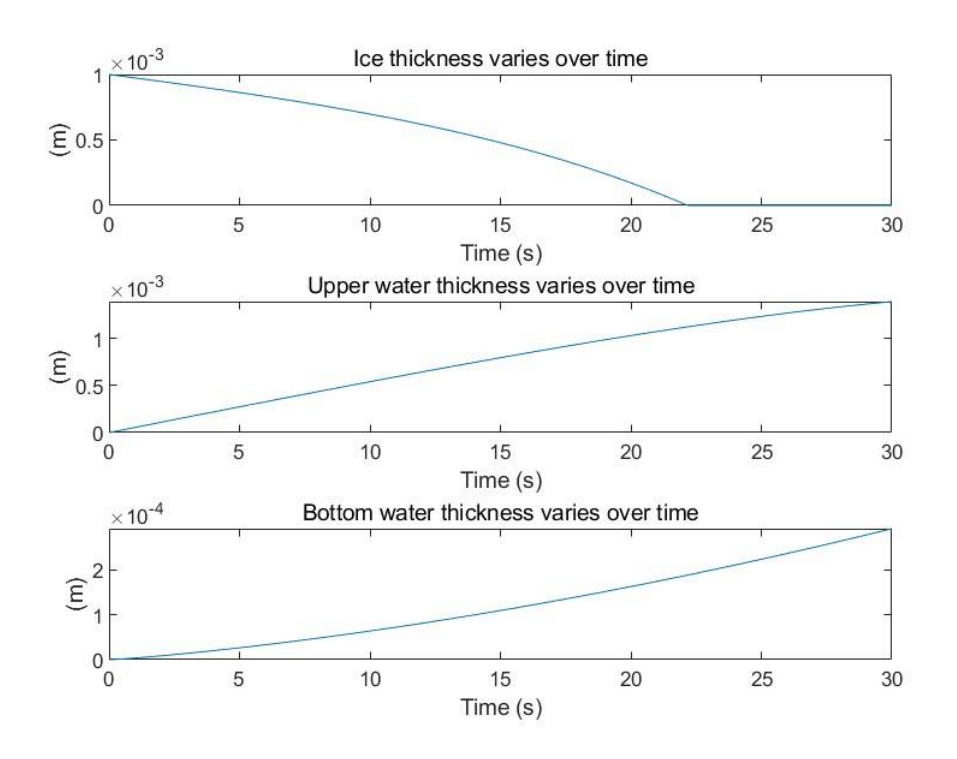


Figure 11 – Environment temperature 0°C

Due to the absence of the upper water layer (freezing while colliding), there is little difference in the thickness of the ice sheet at different temperatures, but there is a difference in the thickness of the lower layer of water, and as the temperature rises, the lower layer of water is thicker, and the ice

TRANSIENT SIMULATION CALCULATION FOR ELECTRIC THERMAL ANTI-ICING PERFORMANCE OF COMPOSITE WING sheet is more likely to break off.

If the temperature difference from the freezing point is very small, there is heat exchange and mass exchange between the three layers, which makes the ice melt faster. This may result in a lower temperature at a higher liquid flow rate and a higher liquid water content, but generally not lower than minus 5°C, depending on the kinetic energy of the droplets, the heat conduction of the ice sheet, and the enthalpy carried by the supercooled water.

3.2.3 Periodic heating

Two kinds of periodic heating were used to observe the effect of anti-icing while maintaining the average heating power of 20kW. The effect is shown in figure 12 and 13.

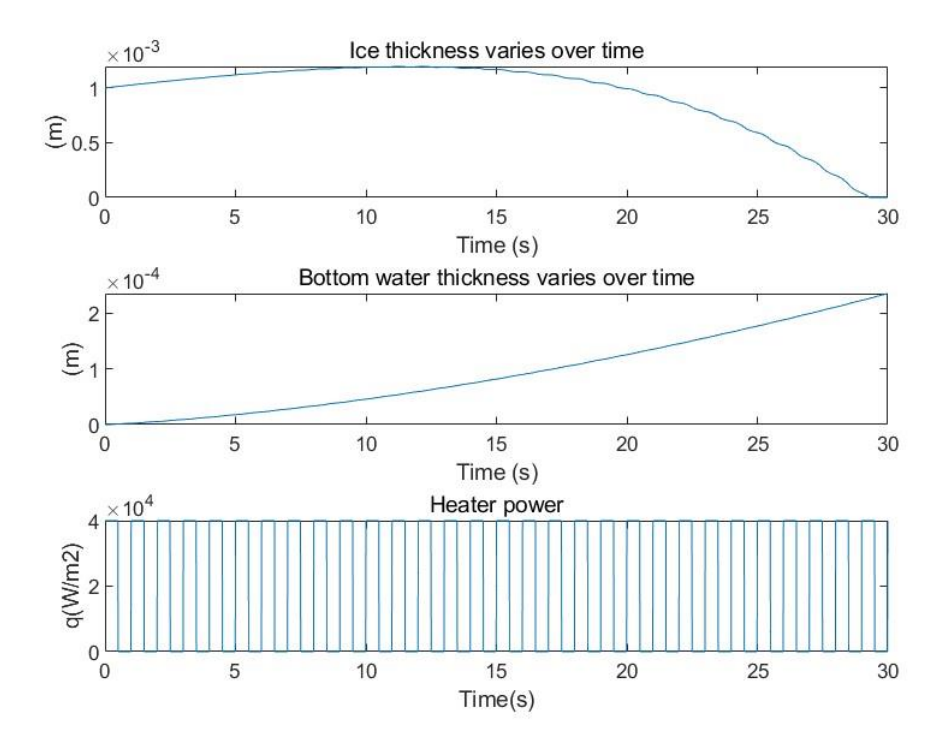


Figure 12 - Periodic heating function 1

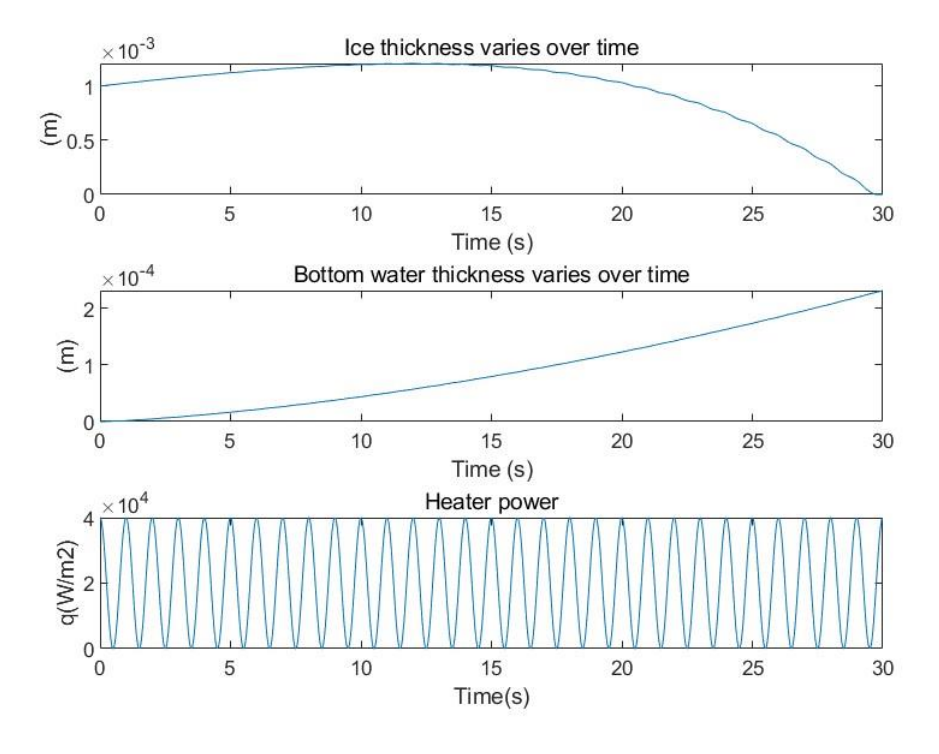


Figure 13 – Periodic heating function 2

TRANSIENT SIMULATION CALCULATION FOR ELECTRIC THERMAL ANTI-ICING PERFORMANCE OF COMPOSITE WING

As can be seen from the above calculation, the use of periodic function electric heating for anti-icing can reduce excessive energy loss to a certain extent, so that the anti-icing effect can be improved to a certain extent, which is reflected in the thickness of the ice sheet and the faster generation speed of the underlying water. In the calculation, we give priority to the initial maximum power, which can make full use of this part of the heat energy quickly corresponding to the melting of the ice.

Next, we study the periodic function of trigonometric function and calculate the anti-icing effect at different frequencies. The result is shown in figure 14 \sim 16, as in figure 13, frequency f = 1.

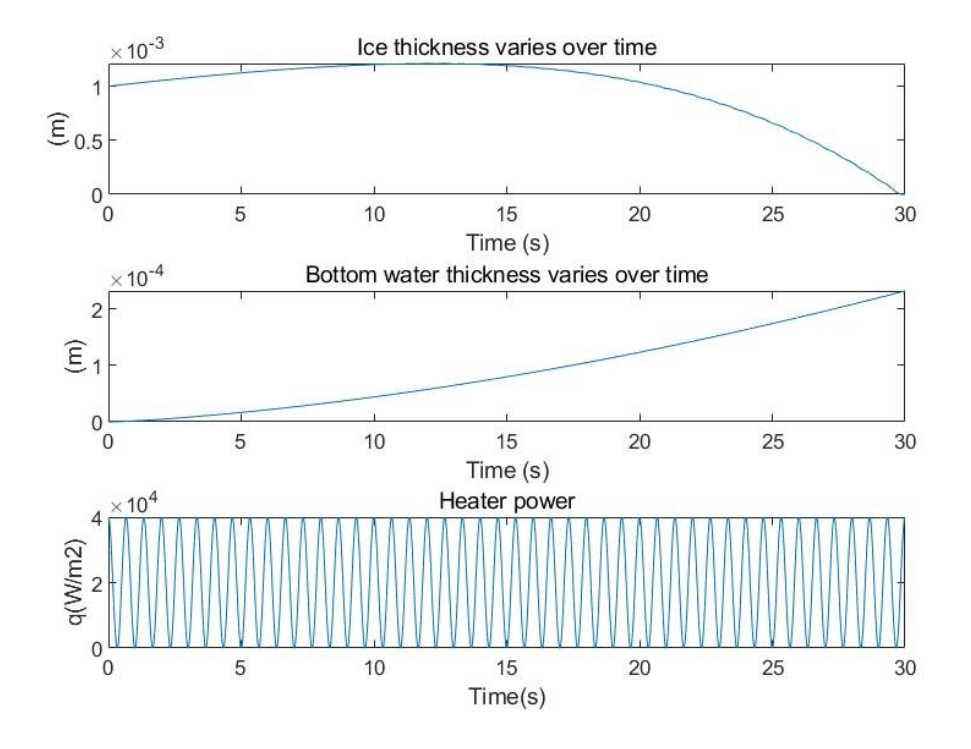


Figure 14 – Heating frequency f = 2

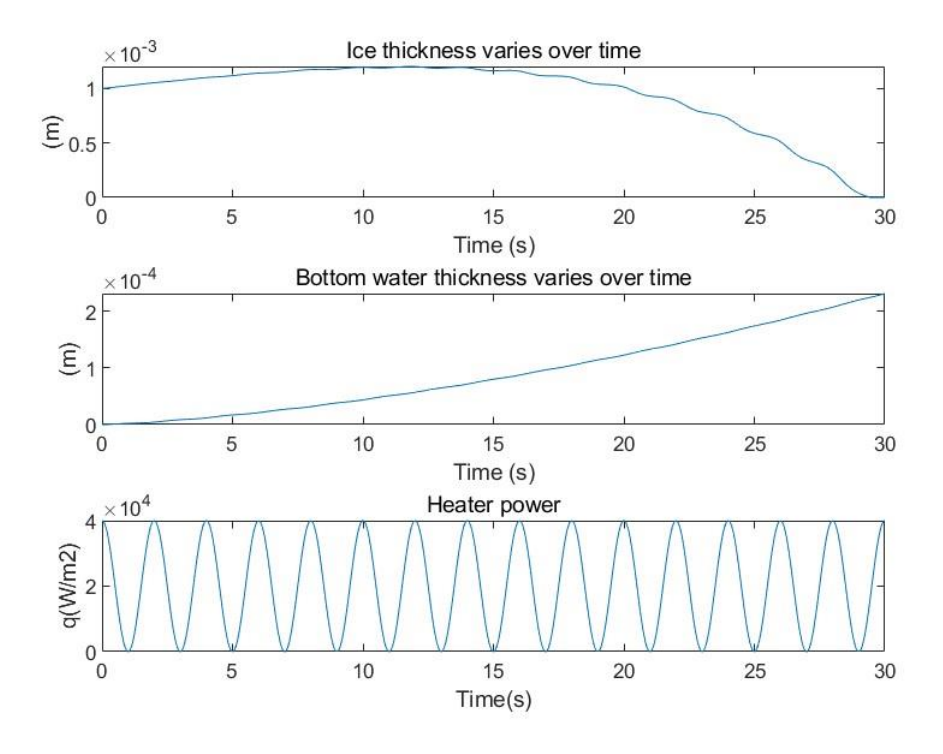


Figure 15 – Heating frequency f = 0.5

It can be seen from the calculation results that with the increase of frequency, the result is more and more close to the result of continuous heating, while at a lower frequency, it can be clearly seen that

TRANSIENT SIMULATION CALCULATION FOR ELECTRIC THERMAL ANTI-ICING PERFORMANCE OF COMPOSITE WING

there is a large gradient velocity decline area, and we can select some of them to compare the corresponding high heating power area, which can quickly achieve the ice melting effect. In practical applications, we can summarize the "heating rate response time" (the interval time between the effect of heating power changes on the ice melt rate, around 1s in this result) so that in practical applications, uniform heating can be given priority, and the power can be increased to accelerate the process near reaching the required conditions, so that the overall energy consumption is close to while the anti-icing rate can be significantly accelerated.

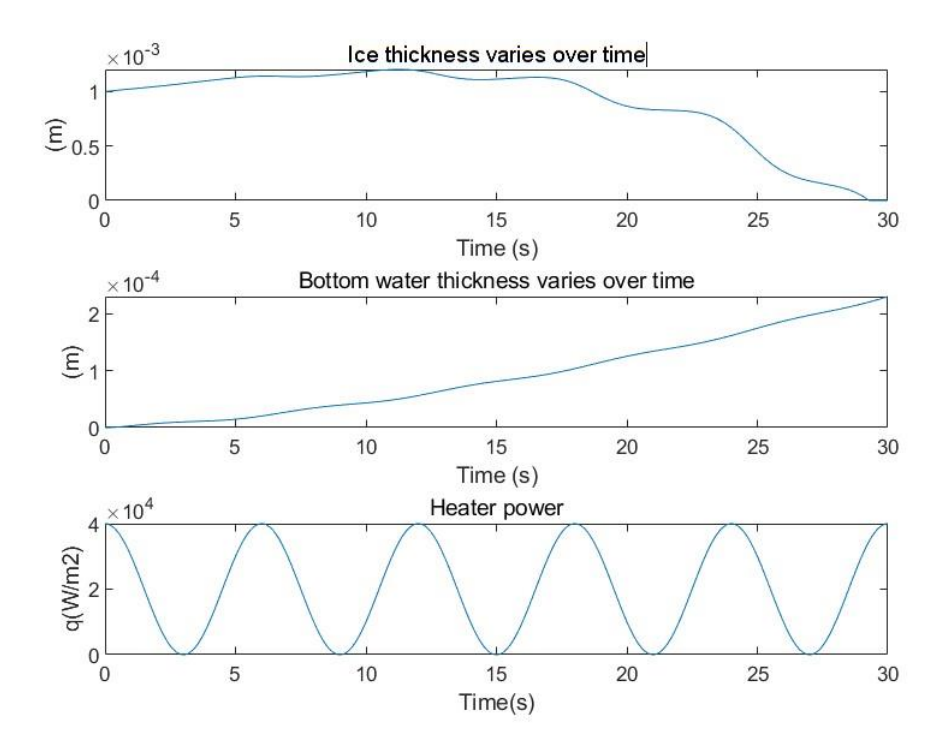


Figure 16 – Heating frequency $f = \frac{1}{6}$

The figure 17 is a comparison of ice layer thickness and bottom water layer thickness at different heating frequencies. It can be clearly seen from the comparison that the thickness of the ice layer is always thinner than that of continuous heating during the heating process at lower frequencies.

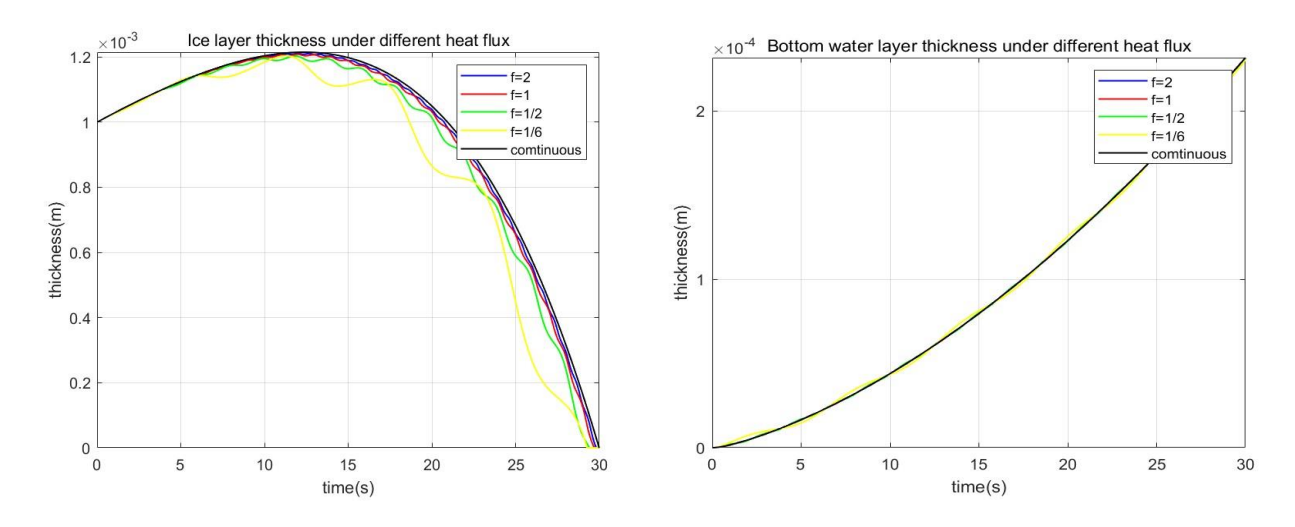


Figure 17 – Comparison of ice and water layer thickness at different heating frequencies

4. Conclusion

The one-dimensional approximation is used to solve the transient anti-icing process. In general environment (except for high liquid water content and temperature close to 0°C, there is liquid water flowing in the upper layer), the melting and freezing process is a dynamic process that gradually melts below the ice layer while the upper layer is still frozen. The content of liquid water significantly affects the thickness of icing, so that the thinner bottom water layer can make the ice layer fall off. The environment temperature mainly affects the thickness of the water layer, but has little effect on the thickness of the ice layer. The influence of environmental temperature on anti-icing is mainly reflected in the growth of the thickness of the underlying water film, and the external thermal conductivity in the lower environment makes the underlying ice not easy to melt. Meanwhile, it is calculated that the periodic heating method can accelerate the ice melting to a certain extent and slightly affect the thickness of the underlying water film, while the reasonable form of long-period heating method may make the optimization effect better. At the same time, the time constant of heating on the ice sheet falling off can be numerically simulated by using the rule of periodic heating and periodic melting of ice layer. It shows that the lag degree of the influence of heating power change on the ice sheet shedding under a certain environment can also design a more reasonable heating method according to different environmental changes.

5. Contact Author Email Address

Pingyang Wang: wangpy@situ.edu.cn

6. Copyright Statement

This document is composed entirely of original content created by the author. No part of the material used herein is subject to copyright infringement. The content has been meticulously researched and developed to ensure that it is free from any proprietary restrictions.

Any references to external works are properly cited and are used in accordance with fair use policies, academic standards, and ethical guidelines. The author guarantees that no copyrighted material has been used without proper authorization or acknowledgment.

If any issues of copyright concern are identified, please contact the author immediately for rectification.

References

- [1] Guo X, Yang Q, Zheng H, et al. Integrated composite electrothermal de-icing system based on ultrathin flexible heating film[J]. Applied Thermal Engineering, 236: 121723, 2024.
- [2] Guo X, Yang Q, Zheng H, et al. Optimization of power distribution for electrothermal anti-icing systems by differential evolution algorithm[J]. Applied Thermal Engineering, 221: 119875, 2023,.
- [3] Xiaofeng Guo, Qian Yang, Haoran Zheng. Effects Of Anisotropic Thermal Conductivity Of Composite Shield On The Electrothermal Anti-Icing Systems. ICAS conference, 2022
- [4] Silva G A L, de Mattos Silvares O, de Jesus Zerbini E J G. Numerical simulation of airfoil thermal antiice operation, part 1: mathematical modelling[J]. Journal of Aircraft, 44(2): 627-633, 2007.
- [5] Silva G A L, Silvares O M, Zerbini E J G J. Numerical simulation of airfoil thermal anti-ice operation, part 2: implementation and results[J]. Journal of aircraft, 44(2): 634-641, 2007.
- [6] Bennani L, Trontin P, Radenac E. Numerical simulation of an electrothermal ice protection system in anti-icing and deicing mode[J]. Aerospace, 10(1): 75, 2023.
- [7] Shen X, Wang H, Lin G, et al. Unsteady simulation of aircraft electro-thermal deicing process with temperature-based method[J]. Proceedings of the Institution of Mechanical Engineers, Part G: Journal of Aerospace Engineering, 234(2): 388-400, 2020.
- [8] Mu Z, Lin G, Shen X, et al. Numerical simulation of unsteady conjugate heat transfer of electrothermal deicing process[J]. International Journal of Aerospace Engineering, 2018(1): 5362541, 2018.
- [9] Ding L, Chang S, Yang S, et al. Study on heating strategies of nose cone electrothermal anti-icing[J]. Journal of Aircraft, 55(3): 1311-1316, 2018.
- [10]Chang S, Zhao Y, Yang B, et al. Study on the Minimum Anti-Icing Energy Based on the Icing Limit State[J]. Journal of Aircraft, 53(6): 1690-1696, 2016.
- [11]Pourbagian M, Talgorn B, Habashi W G, et al. Constrained problem formulations for power optimization of aircraft electro-thermal anti-icing systems[J]. Optimization and Engineering, 16: 663-693, 2015.
- [12]Incropera, F P, & DeWitt, D P. Fundamentals of Heat and Mass Transfer, 6th ed. Wiley. 2006